Potential efficacy of curcumin and curcumin nanoemulsion against experimental cyclosporiasis

Original Article

Nermine MFH Mogahed[1], Maha R Gaafar[1], Thanaa I Shalaby[2], Eman Sheta[3], Fadwa M Arafa[1]

Departments of Medical Parasitology[1], Medical Biophysics[2], and Pathology[3], Faculty of Medicine[1,3], and Medical Research Institute[2], Alexandria University, Alexandria, Egypt

ABSTRACT

Background: There is an urgent need for an effective and safer sulfa-free alternative therapeutic agent considering that trimethoprim-sulfamethoxazole (TMP-SMX), the drug of choice for the treatment of cyclosporiasis, is associated with numerous side effects including bone marrow suppression.
Objective: To evaluate curcumin (CR), and CR nano-emulsion (CR-NE) for their anti-*Cyclospora* potential therapeutic effects compared to the standard treatment in both acute and relapse murine models.
Material and Methods: In a case-control study, 54 male Swiss strain Albino mice received 10^4 sporulated *Cyclospora* oocysts via oral gavage. The experimental groups were treated either with CR, CR-NE, or TMP-SMX. Half of the mice from each group were sacrificed on the 14th d post-infection (dpi), while the remaining mice were left to assess the recurrence of infection on the 30th dpi. Evaluation parameters included stool oocyst load, oocyst ultrastructural changes by scanning electron microscopy (SEM), antioxidant activity, and histopathological changes.
Results: Compared to TMP-SMX, NE formulation increased CR potential effects. In mice receiving CR-NE, a statistically significant decrease in the oocyst burden, and significant improvement in antioxidant biomarkers were evident. Moreover, SEM examination revealed deformed oocysts with irregular outer surfaces, poring, and perforations that were more evident after CR-NE treatment.
Conclusion: It was concluded that CR and CR-NE may be considered novel agents for treating cyclosporiasis and further studies are needed to investigate the pharmacodynamics and pharmacokinetics of CR-NE.

Keywords: antioxidant capacity; curcumin; cyclosporiasis; nano-emulsion; malondialdehyde; therapeutic potential.

Received: 20 September, 2023; **Accepted:** 21 November, 2023.

Corresponding Author: Fadwa M. Arafa; **Tel.:** +20 1146634625**; Email:** f_arafa10@alexmed.edu.eg

Print ISSN: 1687-7942, **Online ISSN:** 2090-2646, **Vol. 16, No. 3, December, 2023.**

INTRODUCTION

Cyclospora is a coccidian protozoan transmitted *via* the fecal-oral route, causing worldwide waterborne outbreaks. Cyclosporiasis is reported in all countries but it is more prevalent in tropical areas[1]. Unsporulated oocysts are shed in the stool of infected patients and sporulate in the environment, becoming infective in a matter of days or weeks. Oocysts maintained under standard laboratory conditions, in deionized water or potassium dichromate, can sporulate in 7-14 d[2]. Numerous cyclosporiasis-induced food-borne outbreaks were recorded in the United States and Canada[3]. In addition, *Cyclospora* has been recovered from Gandofli (*Caelatura Iaronia pruneri*) in Alexandria, Egypt[4]. It has been reported that *C. cayetanensis* is the only species of the genus *Cyclospora* known to infect humans[2]. Conversely, *Cyclospora* spp. oocysts have been found in the feces of several animals, such as dogs, mice, rats, monkeys, ducks, chickens, and other avian species. Furthermore, *Cyclospora* oocysts have been detected in feces of dairy cattle by molecular characterization[2].

Cyclosporiasis is a self-limiting disease in most immunocompetent patients, however, it may present as severe, chronic diarrhea in immunocompromised patients[5]. Diagnosis usually involves microscopic detection of oocysts in stool specimens using modified acid-fast and safranin stains[6]. Unfortunately, *Cyclospora* oocysts are resistant to routine chlorination of water, as well as to commonly used medications against enteric diseases[7]. In spite of considering TMP-SMX a drug of choice for treatment of cyclosporiasis[8], it was allegedly associated with numerous side effects, including bone marrow suppression[9].

Additionally, ciprofloxacin can be used as an alternative therapy in patients with sulfonamide allergies, although it is not as effective as TMP-SMX[10]. Other antibiotics such as azithromycin, nalidixic acid, diloxanide fluorate, tinidazole, norfloxacin, quinacrine were investigated for cyclosporiasis treatment without success[11]. On the other hand, nitazoxanide was used in a clinical trial for the treatment of cyclosporiasis and revealed efficacy ranging from 71-87%[8]. Thus, we

Personal non-commercial use only. PUJ copyright © 2023. All rights reserved DOI: 10.21608/PUJ.2023.237883.1223

are in urgent need of an effective sulfa-free alternative and safer therapeutic agent for the treatment of this infection.

Curcuma longa and its bioactive agent CR have been used in medicine because of their considerable pharmacological properties. Their anti-tumor and anti-inflammatory activities were documented in several studies[12,13]. Additionally, its antioxidant properties have been highlighted[12]. Over the past few years, the anti-protozoal potential of CR was reported in both *in vitro* and in vivo research[13,14]. Nano-emulsions (NEs) are nano-sized preparations with a droplet size ranging from 2 to 200 nm. They are considered new drug delivery systems that enhance the therapeutic efficacy of the drug and minimize its toxic reactions. These NEs are made by combining two immiscible liquids to produce a single phase with the help of an emulsifying agent, surfactant, and co-surfactant. Major applications of NEs involve treatment of reticuloendothelial system infections, chemotherapy, and immunization[15]. Notably, CR-NE was proved effective against *T. gondii* in both acute and chronic infections[16,17]. Therefore, the present study aimed at studying the anti-*Cyclospora*l activity of CR and CR-NE in a murine model of acute cyclosporiasis.

MATERIAL AND METHODS

The current case-control study was conducted at Medical Parasitology Department, Faculty of Medicine, Alexandria University, Alexandria, Egypt during the period from January 2021 to June 2021.

Study design: The 54 mice were divided into control (18) and experimental (36) groups. All mice from non-infected subgroups (Ia) and half of the mice from infected subgroups (Ib, IIa, IIb, and IIc) were sacrificed on the 14th dpi for parasitological, biochemical, and histopathological assessments, while the remaining infected mice from infected subgroups (Ib, IIa, IIb, and IIc) were left to assess the recurrence of infection on the 30th dpi.

Isolation and maintenance of the parasite: *Cyclospora* oocysts were isolated from a fecal sample collected from an HIV positive patient and were successfully stained with modified Ziehl Neelsen (MZN) and safranin stains[18]. The sample was thoroughly examined and confirmed to be *Cyclospora* oocysts by three expert parasitologists. Quality control measures were followed, and a control slide of *C. cayetanensis* from a 10% formalin preserved specimen was included with each staining batch in both staining techniques. The slides stained well in comparison to control slides, and the sample was considered positive when agreeable results were obtained with both stains by at least two observers in a single slide, or when found on different slides of the same sample. The oocysts were left to sporulate, then the mature oocysts were used to infect mice and the cycle was maintained in the Medical Parasitology Department, Faculty of Medicine, Alexandria University. Oocysts were isolated from the stool of previously infected mice by sieving the fecal suspension to remove debris, and washing three times with dechlorinated tap water (2000 rpm for 12 min). Finally, the isolated oocysts were kept in 2.5% aqueous potassium dichromate ($K_2Cr_2O_7$) at 4°C[19].

Sporulation of the isolated oocyst: *Cyclospora* oocysts in 2.5% $K_2Cr_2O_7$ were allowed to sporulate in covered Petri dishes at room temperature (22-30°C). Daily microscopic observation was done until sporulation occurred after 8-14 d. Sporulated oocysts were used later for mice infection[19,20].

Preparation of CR-NE: The NE of CR was prepared using spontaneous emulsification method. For NE preparation, coconut oil was chosen as the oily phase, a mixture of Tween 80 and Tween 85 as surfactants, and ethanol as co-surfactant. Briefly, CR was dissolved in coconut oil by slow addition of surfactant, co-surfactant, and distilled water using constant magnetic stirring at 100 rpm for two hours[21].

Characterization of CR-NE

Transmission electron microscopy (TEM): The size and shape of the prepared CR-NE were determined by TEM (JEOL-100 CX) after NE was diluted with distilled water (1:4), followed by sonication for ten minutes. A drop of the suspension was placed on a 200-mesh carbon-coated copper grid at room temperature. Grids containing the samples were dried in air, negatively stained using 2% uranyl acetate and allowed to dry at room temperature[21].

Particle size analysis and zeta potential measurements: Hydrodynamic particle size, size distribution (polydispersity index, PDI) and zeta potential of CR-NE were measured using Zetasizer based on laser light scattering technique[22].

Experimental animals: Fifty-four male Swiss strain albino mice, weighing 20–25 grams, were purchased and kept in plastic cages under standard conditions (25–27°C, light/dark cycles in 12-h intervals, and free access to drinking water and food pellets) in the animal house of the Medical Parasitology Department, Faculty of Medicine, Alexandria University.

Study groups: Before infection, mice stools were examined by conventional parasitological techniques to exclude the presence of previous infections. Mice were divided into 18 serving as control (group I), and 36 as experimental (group II). The control group was further subdivided into 6 non-infected non-treated mice (Ia), 12 infected nontreated mice (Ib). Mice from the experimental group (group II) were further

subdivided into 12 infected TMP-SMX treated mice (IIa), 12 infected CR treated mice (IIb) and 12 infected CR-NE treated mice (IIc).

Mice from all infected subgroups (Ib, IIa, IIb and IIc) were further subdivided into two equal subgroups (6 mice each). The first six mice were sacrificed on the 14th dpi for parasitological, biochemical and histopathological assessments, while the remaining mice were left to assess the recurrence of infection on the 30th dpi[23].

Mice infection: Each mouse received 10^4 sporulated oocysts in 100 µl of distilled water via oral gavage. Oocysts were first washed three times with distilled water to remove the preservative, centrifuged at 1500 x g for 10 min, and counted with a hemocytometer to adjust the infective dose[19].

Drugs, CR and CR-NE doses: Sutrim©, TMP-SMX obtained from Memphis Co. for Pharm. & Chem. Ind., Cairo, Egypt, was administrated to mice in a dose of 5 mg/kg combined with 25 mg/kg once daily for 7 d starting from the 6th dpi[24], which coincided with the beginning of oocyst shedding. CR and CR-NE administration doses were determined following a pilot study. Three doses were tried: 1, 2 and 4 mg/kg/day orally by the same regimen of the control drug (once daily for 7 d starting from the 6th dpi). The least effective doses of both CR and CR-NE capable of reducing oocyst count in mice stool compared to infected, non-treated control subgroup were determined. Therefore, the dose of 2 mg/kg/d for seven consecutive days starting from the 6th dpi was selected.

Assessment of treatment effect

Oocyst shedding: Fecal samples were collected every four days from each mouse of each infected subgroup from the start of oocyst shedding until the last day of treatment on the 6th, 10th and 14th dpi[25]. Fresh samples were smeared and stained by MZN and safranin stains. The number of oocysts was counted in ten high power microscopic fields per slide and the mean count for each subgroup was calculated[26,27]. The percentage of reduction (%R) of oocyst count in the infected treated subgroups compared to the infected non-treated control subgroup was assessed by the following equation: %R = 100 (C –W/C), where C represents the mean number of oocysts recovered from the stool of infected untreated control subgroup, and W represents the total number of oocysts recovered from each infected treated subgroup[28].

Ultrastructural study: For SEM (Joel JSM- IT 200, Tokyo, Japan), fecal specimens from all infected subgroups were washed with PBS, and collected oocysts were fixed in 2.5% glutaraldehyde. This was followed by washing twice with distilled water, and dehydration in ascending concentration of ethyl alcohol (30–100%). Finally, they were embedded in epoxy resin, placed on aluminum stubs, and coated with 20 nm gold particles[29].

Biochemical parameters: Total antioxidant capacity (TAC) was measured to assess the antioxidant status of small intestinal homogenate of mice from all subgroups sacrificed on the 14th dpi using TAC Colorimetric Assay Kit (biodiagnostic, Egypt). The antioxidants present in the sample eliminate a certain amount of the provided hydrogen peroxide (H_2O_2). Then, the residual H_2O_2 is determined colorimetrically by an enzymatic reaction which involves the conversion to a colored product[30]. Additionally, in order to assess the lipid peroxidation in small intestinal homogenate of mice sacrificed on the 14th dpi, a colorimetric lipid peroxidation assay kit (biodiagnostic, Egypt) was used. Throughout this test, the malondialdehyde (MDA) was measured, and the thiobarbituric acid (TBA) that reacted with MDA. This reaction occurred in an acidic medium at temperature of 95°C for 30 min to form TBA reactive product. Next, the absorbance of the resultant pink product was measured at 534 nm[31].

Histopathological assessment: Six mice from each infected subgroup were euthanized by IV injection of an overdose of thiopental sodium on the 14th dpi while the remaining six mice were euthanized on the 30th dpi to detect the recurrence of infection after cessation of treatment. The duodenum was removed; the remaining parts of intestine were tied at both ends by thread and injected by 10% neutral buffered formalin for better fixation. The tissue samples from each mouse were fixed in 10% neutral buffered formalin, separately, embedded in paraffin, cut into 5 µm thick sections and stained with hematoxylin and eosin (H&E). Histopathologic examination of H&E-stained sections from the small intestine of different subgroups was performed. The villous length was measured from tip to base in 5 different fields. The count of intra-epithelial lymphocytes (IELs) was also assessed at tips of villi. It was calculated by counting the number of lymphocytes per 20 epithelial cells at the tips (mean value of 5 random villi)[32]. Both villous length and IELs counts were done using Leica Application suite (version 4.12.0) image analysis system. Other changes as inflammatory infiltrate severity in lamina propria was assessed as mild, moderate, or severe[33].

Statistical analysis: Data were analyzed using IBM SPSS software package version 20.0. (Armonk, NY: IBM Corp). The Kolmogorov-Smirnov test was used to verify the normality of distribution of variables, then ANOVA was used for comparing the different studied subgroups and followed by Post Hoc test (Tukey) for pairwise comparison. Significance of the obtained results was judged when P <5%[34].

Ethical consideration: The present experimental study was performed according to institutional ethical guidelines. It was approved by the Ethics Committee of

the Faculty of Medicine, Alexandria University, Egypt (Protocol approval number: 0305021). Consideration for the well-being and humane sacrifice of the laboratory animals were incorporated into the design and conduct of the current study.

RESULTS

Characterization of CR-NE: Using TEM, the particles were spherical with an average size of 30 nm (Fig. 1a and 1b). The hydrodynamic particle size, polydispersity index (PDI) and zeta potential (ζ) of CR-NE were determined using Zetasizer (Fig. 1c and 1d). The mean hydrodynamic particle size of CR-NE was found to be 40 nm and with polydispersity index (PDI) of 0.33, thus indicating a narrow and favorable particle size distribution (PDI < 0.5). The respective zeta potential value of CR-NE was -37 mV. High stability of the current CR-NE was observed over a storage period of two months at room temperature.

Assessment of treatment efficacy

Microscopic examination of fecal samples from all infected subgroups revealed MZN and safranin stained *Cyclospora* oocysts. The oocysts were spherical, 8 to 10 µm in diameter in infected control subgroup (Fig. 2a, 2b).

Oocyst load: No statistically significant reduction in oocyst count in stool was recorded between the infected non-treated subgroup of mice (Ib) and all infected treated subgroups (IIa, IIb and IIc) on the 6th dpi. However, the reduction was statistically significant on the 10th, 14th, and 30th dpi. CR-NE-treated subgroup (IIc) showed the highest reduction percentage in oocyst shedding ranging from 49.2% on the 10th dpi to 84% at the end of therapy (14th dpi), and was maintained high even two weeks after cessation of the treatment to reach 97.2% on the 30th dpi. However, no statistically significant difference was noticed between IIa, IIb and IIc on all duration days of the study (Fig. 3, Table 1). On the other hand, for the TMP-SMX treated subgroup (IIa), the percentage of reduction in oocyst shedding was lower than that of subgroup IIc on all duration days of the study. However, two weeks after cessation of the TMP-SMX treatment, oocyst excretion was detected again, and the count increased indicating relapse of the infection (Fig. 3, Table 1).

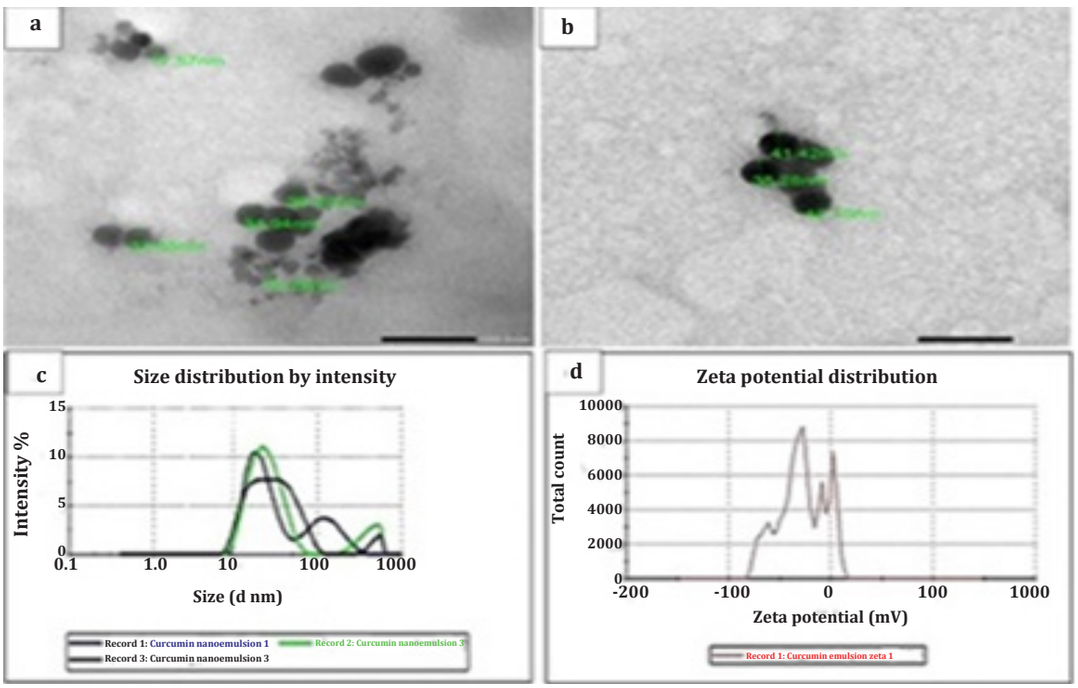

Fig. 1. a, b: TEM of CR-NE studied by TEM (JEOL-100 CX). **c.** Hydrodynamic particle size of CR-NE as measured by Zetasizer. **d.** Zeta potential of CR-NE as measured by Zetasizer.

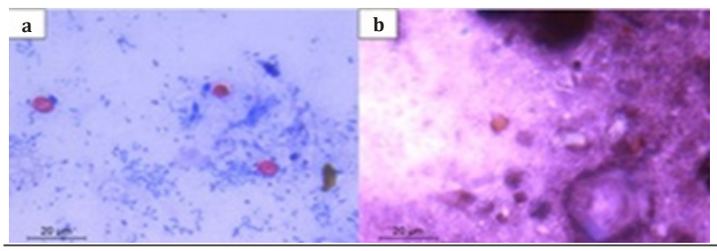

Fig. 2. *Cyclospora* oocysts stained with: a. Modified Ziehl Nielson (MZN). b. Safranin (x1000).

Ultrastructural results: SEM study of oocysts collected from stool sample of subgroup Ib showed ovoid oocysts, about 6x7 µm with smooth outer regular surface (Fig. 4a). On the other hand, those collected from infected mice treated with TMP-SMX exhibited outer surface irregularities and multiple indentations on their surface (Fig. 4b). Other oocysts were enlarged reaching up to 11x12 µm with indentation on one side (Fig. 4c) or with superficial protrusions and indentations (Fig. 4d). Those retrieved from infected mice treated with CR, were distorted with multiple dimples (Fig. 4e) or with superficial irregularities and protrusions (Fig. 4f). Oocysts from infected mice treated with CR-NE were oval and characteristically enlarged in size reaching up to 15 µm in diameter with deep furrows (Fig. 4g). Oocysts from other groups were shrunken to about 4.5x5.5 µm, and were also mutilated with multiple pores and deep furrows (Fig. 4h). Some oocysts of subgroup IIc were enlarged with rough surface irregularities (Fig. 4i). By higher magnification, they appeared as multiple deposits ranging from 26 to 30 nm attached to the external surface (Fig. 4j).

Biochemical results: The level of TAC in subgroup Ib showed statistically significant reduction compared to subgroup Ia. While in both subgroups treated with either CR or CR-NE, TAC was significantly elevated than normal levels. Additionally, they both exhibited

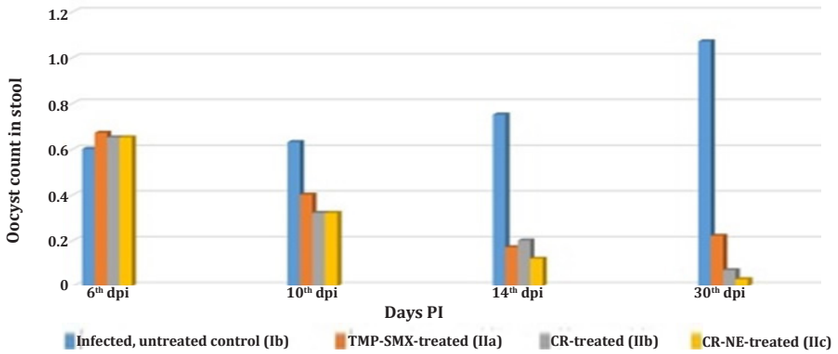

Fig. 3. Comparison between *Cyclospora* oocyst count in stool of different studied subgroups on the 6th, 10th, 14th and 30th dpi.

Table 1. Comparison between *Cyclospora* oocyst counts in stool of different studied subgroups at different durations post infection.

	Ib (n = 6)	IIa (n = 6)	IIb (n = 6)	IIc (n = 6)
6th dpi				
Mean±SD	0.60 ± 0.13	0.67 ± 0.14	0.65 ± 0.14	0.65 ± 0.14
***P*1**		>0.05	>0.05	>0.05
Significance@		***P*1>0.05, *P*2>0.05, *P*3>0.05**		
%R		**45.5**	**47.2**	**47.2**
10th dpi				
Mean±SD	0.63 ± 0.19	0.40 ± 0.06	0.32 ± 0.16	0.32 ± 0.10
***P*1**		0.035*	0.003*	0.003*
Significance@		***P*2=0.716, *P*3=0.716, *P*4=1.000**		
%R		**36.5**	**49.2**	**49.2**
14th dpi				
Mean±SD	0.75 ± 0.12	0.17 ± 0.08	0.20 ± 0.14	0.12 ± 0.08
***P*1**		<0.001*	<0.001*	<0.001*
Significance@		***P*2=0.951, *P*3=0.855, *P*4=0.557**		
%R		**77.3**	**73.3**	**84.0**
30th dpi				
Mean±SD	1.07 ± 0.34	0.22 ± 0.08	0.07 ± 0.08	0.03 ± 0.05
***P*1**		<0.001*	<0.001*	<0.001*
Significance@		***P*2=0.489, *P*3=0.319, *P*4=0.988**		
%R		**79.4**	**93.5**	**97.2**

SD: Standard deviation, ***F***: F for ANOVA test, pairwise comparison between each 2 subgroups was done using Post Hoc Test (Tukey), ***P*1**: *P* value for comparing between Ib and each of the other subgroups; ***P*2**: *P* value for comparing between IIa and IIb; ***P*3**: *P* value for comparing between IIa and IIc; ***P*4**: *P* value for comparing between IIb and IIc; ***:** Statistically significant ($P \leq 0.05$); **@**: Significance between groups. **Ib:** Infected untreated subgroup; **IIa**: Infected TMP-SMX treated subgroup; **IIb:** Infected, CR treated subgroup; **IIc:** Infected, CR-NE treated subgroup.

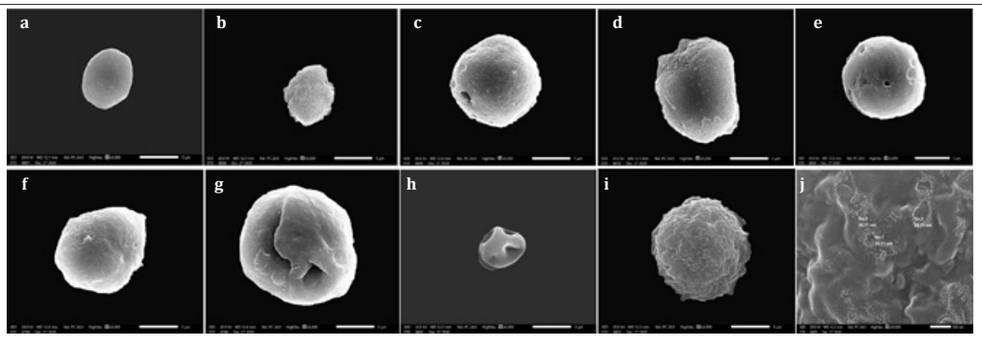

Fig. 4. SEM of *Cyclospora* oocysts in different experimental subgroups on the 14th dpi. **a**. Normal, non-treated ovoid oocyst (~ 6x7 µm) with smooth outer surface (x5000). **b.** TMP-SMX treated oval oocyst (~6x8 µm) with outer surface irregularities and multiple indentations (x5000). **c.** TMP-SMX treated enlarged oocyst reaching 11x12 µm with indentation on one side (x5000). **d.** TMP-SMX treated oocyst with superficial protrusions and indentations (x5000). **e.** CR treated oocyst enlarged in size reaching up to 15 µm in diameter with multiple dimples (x5000). **f.** CR treated oocyst with superficial irregularities and protrusions (x5000). **g.** CR-NE treated enlarged oocyst with deep furrows (x5000). **h.** CR-NE treated oval oocyst shrunken to ~4.5x5.5 µm and mutilated with multiple pores and deep furrows (x5000). **i.** CR-NE treated enlarged oocyst with rough surface irregularities (x5000). **j.** CR-NE treated oocyst with surface irregularities and multiple minute deposits ranging from 26-30 nm and attached to surface (x30000).

statistically significant elevation than those treated with TMP-SMX (Table 2). Besides, MDA in subgroup Ib showed statistically significant reduction compared to subgroup Ia. Meanwhile, none of the infected and treated subgroups (IIa, IIb and IIc) showed statistically significant change compared to subgroup Ia. All treated subgroups also showed significant reduction compared to subgroup Ib with no statistically significant change when compared to each other (Table 2).

Histopathological results: *Cyclospora* infected subgroup (Ib) showed evident blunting and shortening

Table 2. Comparison between the level of TAC and MDA of different studied subgroups on the 14th dpi.

	Control group (I)		Experimental group (II)		
	Ia (n = 6)	**Ib (n = 6)**	**IIa (n = 6)**	**IIb (n = 6)**	**IIc (n = 6)**
TAC (mM/L)					
Mean ± SD	1.23 ± 0.07	0.70 ± 0.14	1.20 ± 0.09	1.60 ± 0.06	1.64 ± 0.10
***P*0**		<0.001*	0.974	<0.001*	<0.001*
***P*1**			<0.001*	<0.001*	<0.001*
Significance@			***P*2<0.001*, *P*3<0.001*, *P*4=0.933**		
% Change		**↓ 43.1**	**↓ 2.4**	**↓ 30.1**	**↓ 33.3**
MDA (nmole/g tissue)					
Mean ± SD	46.3 ± 4.2	95.2 ± 3.0	49.3 ± 4.4	48.3 ± 2.1	44.2 ± 2.9
***P*0**		<0.001*	0.564	0.849	0.809
***P*1**			<0.001*	<0.001*	<0.001*
Significance@			***P*2=0.986, *P*3=0.100, *P*4=0.251**		
% Change		**↑ 105.6**	**↑ 6.5**	**↑ 4.3**	**↑ 4.5**

SD: Standard deviation, ***F***: F for ANOVA test, pairwise comparison between each 2 subgroups was done using Post Hoc Test (Tukey), ***P*1**: *P* value for comparing between Ib and each of the other subgroups; ***P*2**: *P* value for comparing between IIa and IIb; ***P*3**: *P* value for comparing between IIa and IIc; ***P*4**: *P* value for comparing between IIb and IIc; ***:** Statistically significant ($P \leq 0.05$); **@**: Significance between groups. **Ib:** Infected untreated subgroup; **IIa**: Infected TMP-SMX treated subgroup; **IIb:** Infected, CR treated subgroup; **IIc:** Infected, CR-NE treated subgroup.

of villi. The length ranged between 95 and 144 µm, with a mean of 126±26 µm. Evident decreased villous to crypt ratio and foci of surface epithelial erosions were also noticed. Numerous IELs were detected especially at the tips of the villi reaching up to 6–8 lymphocytes per 20 villous tip epithelial cells. Intra-villous vascular spaces were dilated and congested. Crypts showed hyperplasia in the form of increased mitotic activity. Lamina propria showed moderate non-specific lymphoplasmacytic infiltrate (Fig. 5a). Using a higher magnification (x1000), samples from this subgroup showed ruptured intraepithelial sporocysts with released merozoites. They were detected as round and fusiform merozoites in a supranuclear vacuole or on the surface of enterocytes (Fig. 5b). While, at 30 dpi, samples revealed exaggerated features with persistent infection and near total effacement of villous surface (Fig. 5c). Furthermore, higher magnification demonstrated

intraepithelial oocysts in the supranuclear area of the enterocytes (Fig. 5d).

As regards the infected TMP-SMX treated subgroup (IIa), moderate improvement in villous length, which increased to a range of 109-274 µm with a mean of 156±56 µm, was evident during examination. Surface erosions were still noted in some foci (Fig. 5e). IELs were diminished to 3-4 per 20 villous tip epithelial cells. Mild lamina propria lymphoplasmacytic inflammation and edema were still noted (Fig. 6f). At 30 dpi, the same changes were still detected (Fig. 5g, 5h).

At the same time, infected CR treated subgroup (IIb) showed similar changes to subgroup (IIa). The villous length ranged between 141 and 258 µm with a mean of 190±49 µm, and IELs count was 2-4 per villous tip epithelial cells (Fig. 6a, 6b). Those changes were still detected at 30 dpi but the organism was not detected (Fig. 6c, 6d).

Notably, a remarkable improvement in villous length which increased to 215-250 µm with a mean of 233±12 µm in mice receiving CR-NE (subgroup IIc). Intact surface epithelium was also evident. IELs decreased to only 0.5-1 per 20 villous tip epithelial cells. Inflammatory infiltration of lamina propria was mild. Additionally, mild vascular congestion and crypt hyperplasia were still detected. Meanwhile, the organism was not seen by H&E stain (Fig. 6e, 6f). The same findings were still detectable even at 30 dpi (Fig. 6g, 6h).

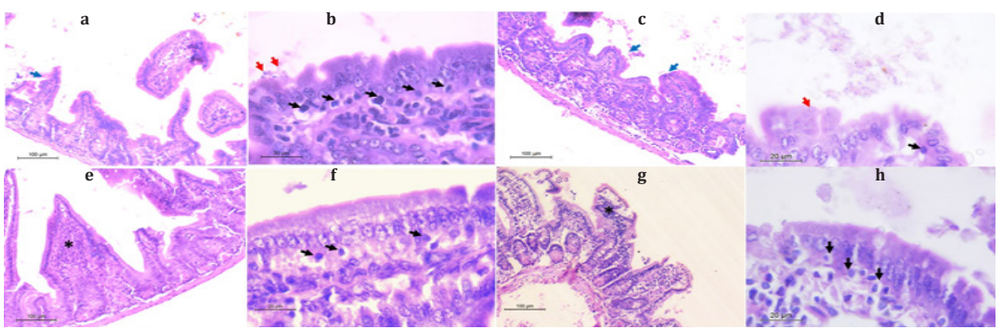

Fig. 5. H&E-stained sections from small intestine of subgroups Ib and IIa. **a.** Infected, untreated control subgroup (Ib) showed blunting of villi and focal erosions (blue arrow) (x200). **b.** Subgroup (Ib) showed numerous IELs (black arrows) and ruptured sporocyst with released merozoites (red arrows) (x1000). **c.** Histologic changes in subgroup (Ib) were exaggerated at 30th dpi with near total blunting of villous surface and frequently seen surface erosions at the tips of villi (blue arrows) (x200). **d.** Subgroup (Ib) at 30th dpi showed IELs (black arrow) and intraepithelial oocyst (red arrow) (x1000). **e.** Infected, TMP-SMX treated subgroup (IIa) showed moderate improvement in villous length with villous mixed inflammatory infiltrate and vascular congestion (asterisk) (x200). **f.** Subgroup (IIa) revealed increased IELs (black arrows) (x1000). **g.** Inflammatory infiltrate was still detected in subgroup (IIa) at 30th dpi (asterisk) (x200). **h.** Subgroup (IIa) at 30th dpi revealed residual IELs (black arrows) (x1000).

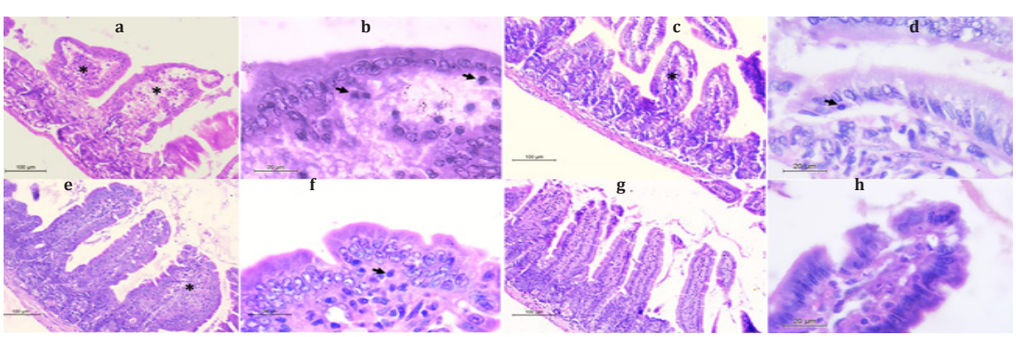

Fig. 6. H&E-stained sections from small intestine of subgroups IIb and IIc. **a.** CR treated subgroup (IIb) showed moderate improvement in villous length. Edema of villi is still seen (asterisk) (x200). **b.** Subgroup (IIb) showed few IELs (black arrows) (x1000). **c.** Inflammatory infiltrate was still detected in subgroup (IIb) at 30 dpi, (asterisk) (x200). **d.** Subgroup (IIb) at 30 dpi revealed few IELs (black arrow) but no parasites were detected (x1000). **e.** CR-NE treated subgroup (IIc) showed maximum improvement of villous length to reach normal level with only mild inflammation and edema (asterisk) (x200). **f.** IELs were seen only focally in subgroup (IIc) (black arrow). No parasites were detected. (x1000). **g.** The histomorphology was much improved in subgroup (IIc) at 30 dpi (x200). The villous length was restored with a normal range of inflammatory cells. **h.** Subgroup (IIc) at 30 dpi showing tip of villi. No ulceration or IELs were noted. Also, no parasites were detected (x1000).

DISCUSSION

Cyclospora cayetanensis is a protozoan with global public health concern. TMP-SMX was considered as the gold standard for its treatment despite the associated various side effects[8]. Over the years, plants and herbs were the main source for drug discovery[35]. Curcumin is a polyphenolic orange–yellow compound. Recently, it attracted considerable attention due to its remarkable pharmacological activities[36]. Anti-protozoal activities of CR have also been documented in *in vitro* studies against *Leishmania*[37]. Additionally, the cytotoxic effect of CR against *G. lamblia* trophozoites was reported. Curcumin inhibited *Giardia* proliferation and adhesion in a time and concentration-dependent mode[38]. Moreover, the anti-protozoal and antioxidant activity of CR against *C. parvum* was also confirmed[13].

The growing interest in human studies on CR is increasing. Apparently, its therapeutic effectiveness depends mainly on the enhanced availability of the drug to target organs, which in turn depends on its adequate aqueous solubility. In contrast with micron-sized emulsions, NEs provide greater surface areas together with the potential of increased solubility. This potential is due to the combined large interfacial adsorption of the core compound, enhanced bioavailability, and improved controlled release of the drug[22,39]. Moreover, CR-NE was found to be a promising treatment for acute and chronic toxoplasmosis, especially in in association with latent bradyzoites in the brain. This may have been due to improved bioavailability, tissue distribution and therapeutic activity of CR-NE compared with CR[22].

Moreover, it was found that the oral route is quite advantageous, since most of the ingested CR remains in the intestinal tract and is eliminated through feces[40]. Thus, its efficiency to kill extracellular intestinal protozoans could be emphasized. Besides, nano-formulation may enhance the bioavailability and prolong the retention time of CR and sustain its effect on intestinal *Cyclospora*[41].

In the current study, the zeta potential values of synthetized CR-NE were highly negative which can increase the stability of particles in suspension by increasing electrostatic repulsion between them. Several studies showed that high positive or negative zeta potentials contribute greatly to the stability of microemulsions and NEs due to the highly charged surfaces, which in turn resist droplet aggregation[22]. Because of their small sizes, NEs remain stable even after storage for long periods[42]. These remarkable properties make CR-NE a highly promising candidate for *Cyclospora* treatment, as proved by the significant reduction in oocyst count observed in all treated subgroups to variable degrees even after complete cessation of treatment. The highest significant reduction in oocyst count was observed in the infected, CR-NE treated subgroup. This was in agreement with Azami *et al*.[22] who noticed a significant reduction in the mean peritoneal tachyzoites count in CR-NE treated mice compared with those treated with CR. In the following year, Gaafar *et al*.[43] proved that silver nanoparticles were an effective treatment against *Cyclospora*. Therefore, it was assumed that CR-NE would produce the same level of effectiveness.

As regards the ultrastructural changes, *Cyclospora* oocysts retrieved from both CR and CR-NE treated subgroups showed the most destructed morphological alterations. Minute particles attached to the surface were also noticed. These were most probably CR-NE particles indicating that they reached their intended target. In agreement with our results, Gutiérrez-Gutiérrez *et al*.[38] reported that CR caused alteration of *G. lamblia* trophozoite ultrastructure. The ventrolateral extension, damage to flagella and caudal region, protrusions and blebs on dorsal and ventral surface were also observed.

Concerning infected mice treated with TMP-SMX, oocysts exhibited outer surface irregularities with multiple indentations and protrusions. Similarly, Gaafar *et al*.[43] reported that *Cyclospora* oocysts treated by TMP-SMX showed abnormal changes on the external surfaces of the treated oocysts. The authors attributed this to the mechanism of action of TMP-SMX which interferes with DNA and proteins synthesis[44].

The anti-parasitic activity of CR was proved in our study by the successful reduction in oocyst count and the appearance of severe ultrastructural changes. It was reported that CR was also highly effective against another apicomplexan protozoa, *C. parvum*, in cell culture. Different studies proved the effectiveness of CR as anti-protozoal agent, however, *C. parvum* appeared to be the most sensitive one[45]. The anti-protozoal activity of CR was explained by several hypotheses. One of these is its effect on the regulation of transcription pathway which needs breaking of chromatin strand that allows entry of transcription factors to DNA. The regulation of this process is maintained through histone acetylation–deacetylation balance, which is under control of histone acetyltransferase (HAT) enzyme. CR has an inhibitory effect on HAT, so it can prevent chromatin remodeling and initiation of transcription pathway of the parasite[46]. Another hypothesis is the induction of cellular apoptosis. This process is initiated through direct stimulation of intracytoplasmic calcium release from intracellular stores leading to elevation of cytosolic calcium[47]. In addition, an increase in the influx of extracellular calcium leads to depolarization of mitochondrial membrane potential, release of cytochrome c starting the apoptotic pathway[48]. At the same time, CR can modulate numerous targets

and cell signaling pathways. These include growth factors, growth factor receptors, transcription factors, cytokines, enzymes, and genes regulating apoptosis. For example, coccidian infection can cause up-regulation of survivin levels within the intestinal cells which is needed to improve parasite survival and replication[13]. It was found that CR can reduce survivin levels in tumor cells, inducing apoptosis[49]. The same mode of action can be used to enhance apoptosis in *Cyclospora*-infected cells.

As regards the TAC assessment, a statistically significant difference in the level of TAC was observed between infected TMP-SMX treated and CR treated either in crude form or NE form in favor of CR. The increase in TAC level in case of CR treated subgroups may be attributed to its being an effective antioxidant and scavenger of various oxygen free radicals such as; hydrogen peroxide, and nitric oxide (NO) which are released from activated macrophages[50].

Malondialdehyde is an important marker used for evaluating the level of oxygen free radicals-induced damage. It was suggested that coccidian infection can cause a status of imbalance between the antioxidant capacity and the production of MDA due to the upsurge in reactive oxygen species (ROS) level following infection which leads to the occurrence of oxidative stress[51]. In the current study, all treated subgroups showed a significant reduction in MDA levels almost reaching the normal level suggesting that the treatment prevented ROS induced damage.

Concerning the histopathological changes in our study, *Cyclospora* infected, untreated subgroup showed evident changes of intestinal villi and crypts. Our results were in agreement with those recorded by other studies[11,33,52]. In one study the investigators reported dramatic changes in the intestinal architecture in biopsies obtained from patients complaining of cyclosporiasis[33]. Field[52] reported parasitophorous vacuoles containing *C. cayetanensis* at various stages of its sexual and asexual life cycle in the apical cytoplasm of the enterocytes overlying the tips of the villi. In our sections of the 30th dpi, specimens revealed exaggerated features with persistent infection and near total effacement of villous surface which is expected due to the chronic nature of the infection.

As regards *Cyclospora* infected TMP-SMX and CR treated subgroups, improvement was evident and IELs were diminished. Meanwhile, mild lamina propria lymphoplasmacytic inflammation and edema were still noted. At the 30th dpi, the same changes were still detected in both subgroups which suggests partial improvement but not complete resolution of infection leading to recurrence after cessation of treatment.

The NE formulation increased the effect of CR. This was proved in the CR-NE treated subgroup (IIc) as shown by the marked improvement of villous length with intact surface epithelium, the diminution in IELs and the inflammatory infiltrates of lamina propria. Meanwhile, the organism was not detected by H&E stain even at the 30th dpi suggesting that the infection was eliminated, and oocyst shedding decreased dramatically with no recurrence after drug withdrawal.

To the best of our knowledge, no histopathological reports about the effect of CR and CR-NE on *Cyclospora* have been published up till now. The current study is the first to evaluate CR and CR-NE as anti-cyclosporiasis therapeutic agents. CR is non-toxic to mammals even at high doses, easily accessible and of low-cost which makes it attractive as a potential antiparasitic drug. Additionally, CR-NE was found to be a novel agent for the treatment of cyclosporiasis especially in immunocompromised patients. At the 30th dpi, recurrence was noticed after cessation of treatment with TMP-SMX and CR, while on the other hand, no recurrence following CR-NE withdrawal was detected. Further studies are needed to investigate pharmacodynamics and pharmacokinetics of CR-NE.

Acknowledgments: The authors appreciate and would like to thank the working staff in the Medical Parasitology Department for their kind support, especially Mrs. Dawlat Ahmed for technical assistance with animal experimentation.

Author contributions: Mogahed NMFH conceptualized the idea of the work, performed the parasitological study, analyzed the data, and wrote the manuscript. Gaafar MR shared in the conceptualization of the idea of the work, supervised the parasitological study, analyzed the data, and edited the manuscript. Shalaby TI prepared and characterized the nanoparticles. Sheta E performed the pathological study, and analyzed the data. Arafa FM performed the parasitological study, analyzed the data, and wrote the manuscript. All authors approved the final manuscript before publication.

Conflict of Interest: The authors declare no conflict of interest.

Funding statement: This research did not receive any specific grant from funding agencies in the public, commercial, or not-for-profit sectors.

REFERENCES

1. Cama VA, Ortega YR. *Cyclospora cayetanensis*. In: Ortega YR, Sterling CR (Eds). Foodborne Parasites. 2nd ed. Berlin/ Heidelberg, Germany: Springer; 2018;41–56.
2. Almeria S, Cinar HN, Dubey JP. *Cyclospora cayetanensis* and cyclosporiasis: An Update. Microorganisms 2019; 7(9):317.
3. Hadjilouka A, Tsaltas D. *Cyclospora cayetanensis*: Major outbreaks from ready to eat fresh fruits and vegetables. Foods 2020; 9(11):1703.
4. Chacin-Bonilla L, Santin M. *Cyclospora cayetanensis* infection in developed countries: Potential endemic foci? Microorganisms 2023; 11(3):540.

5. Alkorta M, Manzanal A, Zeberio I. A case of severe diarrhoea caused by *Cyclospora cayetanensis* in an immunocompromised patient in northern Spain. Access Microbiol 2022; 4(2):000313.
6. Bilung LM, Tahar AS, Yunos NE, Apun K, Lim YA-L, Nillian E, *et al*. Detection of *Cryptosporidium* and *Cyclospora* oocysts from environmental water for drinking and recreational activities in Sarawak, Malaysia. BioMed Res Int 2017; 2017:4636420.
7. Ahmad H, Sinha S. Cyclosporiasis: An emerging potential threat for water contamination. In: Singh PP, Sharma V (Eds). Water and Health. Springer, New Delhi, India; 2014; 179-189.
8. Li J, Cui Z, Qi M, Zhang L. Advances in cyclosporiasis diagnosis and therapeutic intervention. Front Cell Infect Microbiol 2020; 10:43.
9. Parajuli P, Ibrahim AM, Siddiqui HH, Lara Garcia OE, Regmi MR. Trimethoprim-sulfamethoxazole induced pancytopenia: A common occurrence but a rare diagnosis. Cureus 2019; 11(7):e5071.
10. Li J, Wang R, Chen Y, Xiao L, Zhang L. *Cyclospora cayetanensis* infection in humans: Biological characteristics, clinical features, epidemiology, detection method and treatment. Parasitology 2020; 147(2):160-170.
11. Ortega YR, Sanchez R. Update on *Cyclospora cayetanensis*, a food-borne and waterborne parasite. Clin Microbiol Rev 2010; 23(1):218-234.
12. Fuloria S, Mehta J, Chandel A, Sekar M, Rani NNIM, Begum MY, *et al*. A comprehensive review on the therapeutic potential of *Curcuma longa* Linn. in relation to its major active constituent curcumin. Front Pharmacol 2022; 13.
13. Jamil SNH, Ali AH, Feroz SR, Lam SD, Agustar HK, Abd Razak MRM, *et al*. Curcumin and its derivatives as potential antimalarial and anti-inflammatory agents: A review on structure-activity relationship and mechanism of action. Pharmaceuticals (Basel) 2023; 16(4):609.
14. Asadpour M, Namazi F, Razavi SM, Nazifi S. Comparative efficacy of curcumin and paromomycin against *Cryptosporidium parvum* infection in a BALB/c model. Vet Parasitol 2018; 250:7-14.
15. Jaiswal M, Dudhe R, Sharma PK. Nanoemulsion: An advanced mode of drug delivery system. 3 Biotech 2015; 5(2):123-127.
16. Rageh EA, Abaza SM, El-Gayar EK, Alabbassy MM. Assessment of the prophylactic and therapeutic effects of curcumin nanoemulsion in comparison with Spiramycin in mice simulating acute infection with *T. gondii* (RH strain). PUJ 2022; 15(2):154-161.
17. Rageh EA, Abaza SM, El-Gayar EK, Barakat AM, Alabbassy MM. The therapeutic efficacy of curcumin nanoemulsion versus Spiramycin in *Toxoplasma gondii* (ME49 strain) chronically infected mice. PUJ 2022; 15(2):174-180.
18. Abou-El-Naga IF, Gafaar MR. Auamin- phenol VS modified kinyoun's acid fast stains for detection of coccidian parasites. Lab Med 2014; 45(1):65-73.
19. Khalifa AM, El Temsahy MM, Abou-El-Naga IF. Effect of ozone on the viability of some protozoa in drinking water. J Egypt Soc Parasitol 2001; 31(2):603-616.
20. Smith HV, Paton CA, Mitambo MM, Girdwood RW. Sporulation of *Cyclospora* sp. oocysts. Appl Environ Microbiol 1997; 63(4):1631-1632.
21. Bouchemal K, Briancon S, Perrier E, Fessi H. Nano-emulsion formulation using spontaneous emulsification: Solvent, oil and surfactant optimisation. Int J Pharm 2004; 280(1-2):241-251.
22. Azami SJ, Teimouri A, Keshavarz H, Amani A, Esmaeili F, Hasanpour H, *et al*. Curcumin nanoemulsion as a novel chemical for the treatment of acute and chronic toxoplasmosis in mice. Int J Nanomedicine 2018; 13: 7363-7374.
23. Abou-El-Naga IF, Gaafar MR, Gomaa MM, Khedr SI, Achy S. *Encephalitozoon intestinalis*: A new target for auranofin in a mice model. Med Mycol 2020; 58(6):810-819.
24. Madico G, McDonald J, Gilman RH, Cabrera L, Sterling CR. Epidemiology and treatment of *Cyclospora cayetanensis* infection in Peruvian children. Clin Infect Dis 1997; 24(5):977-981.
25. Al-Mathal EM, Alsalem AM. Pomegranate (*Punica granatum*) peel is effective in a murine model of experimental *Cryptosporidium parvum*. Exp Parasitol 2012; 131(3):350-357.
26. Clarke SC, McIntyre M. Modified detergent Ziehl-Neelsen technique for the staining of *Cyclospora cayetanensis*. J Clin Pathol 1996; 49(6):511-512.
27. Ma P, Soave R. Three-step stool examination for cryptosporidiosis in 10 homosexual men with protracted watery diarrhea. J Infect Dis 1983; 147(5): 824-828.
28. Penido ML, Nelson DL, Vieira LQ, Coelho PM. Schistosomicidal activity of alkylaminooctane-thiosulfuric acids. Mem Inst Oswaldo Cruz 1994; 89(4):595-602.
29. Klainer AS, Betsch CJ. Scanning-beam electron microscopy of selected microorganisms. J Infect Dis 1970; 121(3):339-343.
30. Koracevic D, Koracevic G, Djordjevic V, Andrejevic S, Cosic V. Method for the measurement of antioxidant activity in human fluids. J Clin Pathol 2001; 54(5):356-361.
31. Ohkawa H, Ohishi N, Yagi K. Assay for lipid peroxides in animal tissues by thiobarbituric acid reaction. Anal Biochem 1979; 95(2):351-358.
32. Serra S, Jani PA. An approach to duodenal biopsies. J Clin Pathol 2006; 59(11):1133-1150.
33. Ortega YR, Nagle R, Gilman RH, Watanabe J, Miyagui J, Quispe H, *et al*. Pathologic and clinical findings in patients with cyclosporiasis and a description of intracellular parasite life-cycle stages. J Infect Dis 1997; 176(6):1584-1589.
34. Kirkpatrick LA, Feeney BC. A simple guide to IBM SPSS statistics for version 20.0. Belmont, California: Wadsworth, Cengage Learning; 2013.
35. Nasim N, Sandeep IS, Mohanty S. Plant-derived natural products for drug discovery: current approaches and prospects. Nucleus 2022; 65(3):399-411.

36. Amalraj A, Pius A, Gopi S, Gopi S. Biological activities of curcuminoids, other biomolecules from turmeric and their derivatives: A review. J Tradit Complement Med 2017; 7(2):205-233.
37. Kumar M, Pal K, Pratap V, Gour JK. Antileishmanial potential of different extracts of *Curcuma longa* rhizome against *Leishmania donovani*. J Sci Res 2022; 66:129-141.
38. Gutiérrez-Gutiérrez F, Palomo-Ligas L, Hernández-Hernández JM, Pérez-Rangel A, Aguayo-Ortiz R, Hernández-Campos A, *et al*. Curcumin alters the cytoskeleton and microtubule organization on trophozoites of *Giardia lamblia*. Acta Trop 2017; 172:113-121.
39. Lovelyn C, Attama A. Current state of nanoemulsions in drug delivery. J Biomater Nanobiotechnol 2011; 2(5):626-639.
40. Scazzocchio B, Minghetti L, D'Archivio M. Interaction between gut microbiota and curcumin: a new key of understanding for the health effects of curcumin. Nutrients 2020; 12(9):2499.
41. Gera M, Sharma N, Ghosh M, Huynh DL, Lee SJ, Min T, *et al*. Nanoformulations of curcumin: an emerging paradigm for improved remedial application. Oncotarget 2017; 8(39):66680-66698.
42. Hernández-Jaimes C, Fouconnier B, Pérez-Alonso C, Munguía-Guillén JL, Vernon-Carter EJ. Antioxidant activity degradation, formulation, optimization, characterization, and stability of *Equisetum arvense* extract nanoemulsion. J Disper Sci Technol 2013; 34(1):64-71.
43. Gaafar MR, El-Zawawy LA, El-Temsahy MM, Shalaby TI, Hassan AY. Silver nanoparticles as a therapeutic agent in experimental cyclosporiasis. Exp Parasitol 2019; 207:107772.
44. Deshmukh R, Harwansh RK, Sharma M, Paul SD. Novel delivery approaches of co-trimoxazole for recreating its potential use: A review. Int J Appl Pharm 2021:36-42.
45. Ranasinghe S, Zahedi A, Armson A, Lymbery AJ, Ash A. *In vitro* susceptibility of *Cryptosporidium parvum* to plant antiparasitic compounds. Pathogens 2022; 12(1):61.
46. Hassan FU, Rehman MS, Khan MS, Ali MA, Javed A, Nawaz A, *et al*. Curcumin as an alternative epigenetic modulator: Mechanism of action and potential effects. Front Genet 2019; 10:514.
47. Kim E, Lee DM, Seo MJ, Lee HJ, Choi KS. Intracellular Ca2+ imbalance critically contributes to paraptosis. Front Cell Dev Biol 2021; 8:607844.
48. Bagheri H, Ghasemi F, Barreto GE, Rafiee R, Sathyapalan T, Sahebkar A. Effects of curcumin on mitochondria in neurodegenerative diseases. Biofactors 2020; 46(1):5-20.
49. Pandey A, Vishnoi K, Mahata S, Tripathi SC, Misra SP, Misra V, *et al*. Berberine and curcumin target survivin and STAT3 in gastric cancer cells and synergize actions of standard chemotherapeutic 5-Fluorouracil. Nutr Cancer 2015; 67(8):1295-306.
50. Boroumand N, Samarghandian S, Hashemy SI. Immunomodulatory, anti-inflammatory, and antioxidant effects of curcumin. J Herbmed Pharmacol 2018; 7(4):211-219.
51. Yilmaz S, Mustafa I, Kandemir FM, Yusuf G. Malondialdehyde and total antioxidant levels and hematological parameters of beef cattle with coccidiosis. Van Vet J 2014; 25(2):41-45.
52. Field AS. Light microscopic and electron microscopic diagnosis of gastrointestinal opportunistic infections in HIV-positive patients. Pathology 2002; 34(1):21-35.